



HAL
open science

Comparative study of layered material models

Mégane Bati, Romain Pacanowski, Pascal Barla

► **To cite this version:**

Mégane Bati, Romain Pacanowski, Pascal Barla. Comparative study of layered material models. Workshop on Material Appearance Modeling, Jul 2019, Strasbourg, France. hal-02184562

HAL Id: hal-02184562

<https://hal.science/hal-02184562v1>

Submitted on 16 Jul 2019

HAL is a multi-disciplinary open access archive for the deposit and dissemination of scientific research documents, whether they are published or not. The documents may come from teaching and research institutions in France or abroad, or from public or private research centers.

L'archive ouverte pluridisciplinaire **HAL**, est destinée au dépôt et à la diffusion de documents scientifiques de niveau recherche, publiés ou non, émanant des établissements d'enseignement et de recherche français ou étrangers, des laboratoires publics ou privés.

Comparative Study of Layered Material Models

Mégane Bati^{1,4,2},

Romain Pacanowski^{2,1,4} Pascal Barla³

¹Institut d'Optique Graduate School ⁴Université de Bordeaux ²CNRS ³INRIA

Abstract

The accurate reproduction of layered materials is an important part of physically-based rendering applications. Since no exact analytical model exists for any configuration of layer stacks, available models make approximations. In this paper, we propose to evaluate them with a numerical approach: we simulate BRDFs and BTDFs for layered materials in order to compare existing models against a common reference. We show that: (1) no single model always outperforms the others and (2) significant differences remain between simulated and modeled materials. We analyse the reasons for these discrepancies and introduce immediate corrections.

Categories and Subject Descriptors (according to ACM CCS): I.3.7 [Computer Graphics]: Three-Dimensional Graphics and Realism—Color, shading, shadowing, and texture

1. Motivation

Most materials are made of layers, which makes the modeling of surface scattering challenging. Only a few analytical layered material models exist in the literature, with the aim of reaching the highest physical accuracy while remaining in geometric optics. Thus, the impact of approximations made by such models remains unclear.

In this paper, we want to determine which layered material models provide the best results in which configurations. An extended version of our analysis is available as technical report [BPB19]. We draw our inspiration from the study of Ngan et al. [NDM05], comparing models to measured materials. Here, our ground truth is given by path tracing (geometric optics assumptions), and we focus on three classes of materials and two models, each declined in two variants. In Section 4, we analyze the design choices leading to inaccuracies and make immediate corrections.

Layered models Previous work on layered models often consider layers to consist of either plane-parallel interfaces or media. Except for stacks of perfectly smooth interfaces [Yeh05], no exact solution is known. Hence existing models necessarily make assumptions and simplifications.

The model of Weidlich and Wilkie [WW07] recursively combines arbitrary BRDFs of successive interfaces, while handling absorption in media through the Beer-Lambert law. The opaque base layer may be defined with any BRDF. The model is simple and versatile, but limited to the modeling of BRDFs and does not consider multiple scattering.

In contrast, the method of Guo et al. [GQGP17] han-

dles BTDFs and accounts for the main inter-reflections. The model is limited to transparent media bounded by rough interfaces, defined by von Mises-Fisher distributions.

Belcour [Bel18] takes a similar approach, proposing a statistical representation that accomodates GGX distributions for interfaces. The method works as if a bundle of rays were traced through the stack, with its statistics (energy, mean and variance) updated at each event (reflection, refraction, absorption and forward scattering). It handles inter-reflections among layers through an extended adding procedure.

Numerical techniques When physical accuracy is of primary interest, one may simulate the light transport in a layered material, with the downside of increasing rendering times. Guo et al. [GHZ18] proposed a solution relying on a position-free light transport simulation in the layer stack.

An alternative is the Layer Lab system [JdJM14] which combines layers expressed in a sparse Fourier-based representation. The method is efficient for modeling rough interfaces and participating media, but requires longer precomputation times and storage when smoother interfaces are involved; ringing artifacts may appear otherwise. The representation is adapted to Beckmann interfaces, but GGX interfaces require a look-up table in the MERL format. To the best of our knowledge, this only works for reflection; hence such interfaces may only be used as opaque bases.

2. Models

We compare layered material models that can handle GGX distributions [WMLT] that rely on microfacet theory [TS67];

a BRDF is then defined as:

$$f_r(\mathbf{l}, \mathbf{v}) = \frac{D(\mathbf{h})G(\mathbf{l}, \mathbf{v})F(\mathbf{l} \cdot \mathbf{h})}{4|\mathbf{l} \cdot \mathbf{n}||\mathbf{v} \cdot \mathbf{n}|}, \quad (1)$$

where D is the microfacet distribution, G is the geometric attenuation, F is the Fresnel reflectivity, \mathbf{l} is the incoming (or light) direction, \mathbf{v} is the outgoing (or view) direction, \mathbf{n} is the geometric normal and $\mathbf{h} = \frac{\mathbf{l} + \mathbf{v}}{\|\mathbf{l} + \mathbf{v}\|}$ is the half-way vector.

2.1. Weidlich & Wilkie's model and variants

The model of Weidlich and Wilkie [WW07] accomodates any type and number of interfaces through a recursive approach. Focusing on a pair of interfaces, it is defined as:

$$f_r^{ww}(\mathbf{l}_0, \mathbf{v}_0) = f_{r_0}(\mathbf{l}_0, \mathbf{v}_0) + T_{01} f_{r_1}(\mathbf{l}_1, \mathbf{v}_1) at; \quad (2)$$

with $a = e^{-\sigma_a d \left(\frac{1}{|\mathbf{n} \cdot \mathbf{l}_1|} + \frac{1}{|\mathbf{n} \cdot \mathbf{v}_1|} \right)}$ and $t = (1 - G) + T_{10}G$. The layered BRDF f_r^{ww} is obtained as a combination of the BRDFs f_{r_0} and f_{r_1} characterizing the top and bottom interfaces. While the former is evaluated in the directions \mathbf{l}_0 and \mathbf{v}_0 , the latter uses the transmitted directions \mathbf{l}_1 and \mathbf{v}_1 , and is attenuated by: the Fresnel transmissivity T_{01} ; Beer-Lambert attenuation a based on the absorption coefficient σ_a and layer depth d ; an approximation t of the effect of total internal reflection (TIR) based on the geometric attenuation factor G from microfacet theory. The recursion is applied to f_{r_1} through Equation 2 when more layers are considered.

A subtle approximation lies in the choice of the interface normal used for computing Fresnel transmissivity as well as \mathbf{l}_1 and \mathbf{v}_1 through Snell's law: one may either use the geometric normal \mathbf{n} or the half-way vector \mathbf{h}_0 (i.e., the top microfacet normal). Different solutions have been chosen in two variants of the model [WW09, Ele10]. Although they both rely on \mathbf{h}_0 for computing transmissivity, they differ in the way they compute the refracted vectors. Perhaps surprisingly, the variant of the authors [WW09] does not make use of the refracted directions ($\mathbf{l}_1, \mathbf{v}_1$) when evaluating the BRDF f_{r_1} of the bottom interface. Additionally, the variant of Elek uses a modified base roughness: $\alpha_1 \leftarrow \max(\alpha_0, \alpha_1)$. In a recent variant [WW11], a similar modification is proposed, specific to the Blinn distribution, thus not considered here.

2.2. Belcour's models

The approach of Belcour [Bel18] expresses a layered BRDF as the sum of K GGX lobes (K is the number of layers):

$$f_r^b(\mathbf{l}_0, \mathbf{v}_0) = \sum_{k=0}^{K-1} e_k(\mathbf{l}_0) \rho_k(\mathbf{l}_0, \mathbf{v}_0; \alpha_k(\mathbf{l}_0)), \quad (3)$$

where e_k stands for the directionally-dependent energy of the k -th lobe, and ρ_k is of the form of Equation 1, except that the roughness α_k of the GGX distribution D is allowed to vary with the incoming direction. Each lobe is implicitly pointing in the direction of the reflected incoming direction;

hence only e_k and α_k must be computed from the physical parameters of the layer stack. This is done by first tracking ray bundles and updating their directional statistics with atomic operators, then combining layers by an extended version of the adding procedure, which handles inter-reflections among layers (see the paper for details). Even though Belcour's model does handle scattering, it is *limited to forward propagation*, meaning that a bundle of rays entering a base scattering medium will never exit the surface on reflection.

The model makes a number of approximations. The energy e_k must be updated at an interface layer according to both Fresnel reflectance and roughness. This is made possible by precomputing the directional albedo of the BRDF of an interface – called FGD – and making the approximation that it is decoupled from incident radiance. Note that Belcour uses a precomputed FGD^∞ that accounts for inter-reflections at the interface; however, due to numerical issues potentially violating energy conservation, we do not consider that solution. The roughness α_k is not directly updated in the propagation of a ray bundle: its variance is. A mapping between the GGX roughness parameter and the variance is thus employed, which might include further approximations.

This *forward* model has another limitation: it is not reciprocal. Belcour suggests a *symmetric* model, whereby the half-way vector at the top interface \mathbf{h}_0 is used in place of the geometric normal \mathbf{n} when updating statistics. Both e_k and α_k then become symmetric across a flip of \mathbf{l}_0 with \mathbf{v}_0 , which makes the BRDF reciprocal. This symmetrization assumes that \mathbf{l}_0 and \mathbf{v}_0 share the same microfacet, and its normal \mathbf{h}_0 will be used at all subsequent occurring events.

3. Evaluation

3.1. Methodology

We have implemented a virtual gonio-spectrophotometer to evaluate the impact of the model approximations described in the previous section. Our light transport simulation relies on a Monte-Carlo path-tracer: rays are sent onto the layer stack from one incoming direction; they propagate by unidirectional path tracing until they exit the stack either by reflection or transmission; they are finally accumulated in a hemisphere of directions and their density is used to compute either a BRDF or BTDF slice. Several slices constitutes a raw simulated BRDF. To perform the comparison with models, we integrated their response on the same slice parametrization, which is the data used in the following.

We consider three material categories: plastics, metals and transparent slabs. They share the same top interface: a GGX coating layer of roughness α_0 , with a constant index of refraction η_0 and an optical depth (colored or achromatic), defined as $\tau = \sigma_a d$ as we only rely on Beer-Lambert law for media. Plastics use a Lambertian base layer of albedo ρ (colored or achromatic). Metals are obtained by using a conductor base layer, with index of refraction $\eta_1 + i\kappa_1$ (only η_1

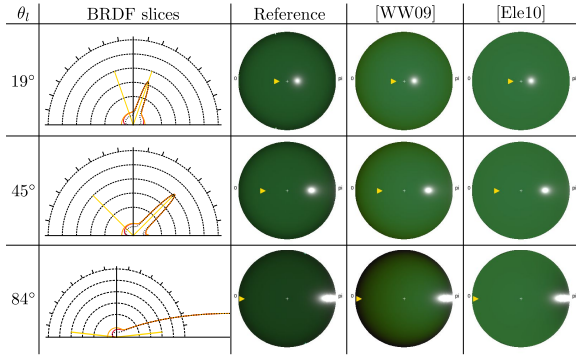


Figure 1: Results for a plastic material ($\alpha_0 = 0.05$, τ and ρ colored). We remap values using $\log(1 + \sqrt{f_r})$. The reference is the dashed black curve, whereas models are represented in color (red [WW09], orange [Ele10]). The last columns show the slice with a top orthographic view, the light direction being in yellow. The models over-estimate diffuse lobe intensity and differ in color and shape with the reference.

varies) and a roughness α_1 . Transparent slabs are achieved with a dielectric base layer of index 1.0 and a roughness α_1 .

3.2. Results

Plastics Only the variants of Weidlich and Wilkie’s model accommodate this category. As expected, in Figure 1, the specular peaks of the two variants match, but their diffuse lobes differ in intensity, color and shape, both from the reference and each others. The models overestimate the diffuse intensities, even though they ignore inter-reflections in the layer stack. Elek’s model reasonably preserves the greenish color resulting from the choice of a colored diffuse base and a slightly absorptive coating layer; whereas the model of Weidlich and Wilkie produces a more yellowish color. The shapes of the diffuse lobes differ from the reference: they are not radially-symmetric around the normal \mathbf{n} (noticeable at grazing angles) and show only slight variations with α_0 .

Metals As before, Weidlich and Wilkie’s variants are exact for reflection off the first interface unlike Belcour’s. In Figure 2, we show a metallic paint: a smooth coating on top of a rough base. The model of Weidlich and Wilkie exhibits an extra achromatic lobe at grazing angles, likely due to its use of non-refracted vectors to evaluate the base layer. Elek’s model does not make this approximation, and as a result is devoid of such artefacts. The models of Belcour produce results similar to Elek’s in this case: they all tend to slightly overestimate the angular spread of the wide reddish lobe due to reflection off the conductor base layer.

In Figure 3, we show a frosted metal: a rough coating on a smooth base. This is the most problematic configuration for Weidlich and Wilkie’s model, which ignores the roughness of the coating layer, resulting in an overly sharp lobe shape

(i.e., a reddish BRDF peak). Elek’s variant corrects this issue by modifying α_1 , but this is not sufficient: the shape of the lobe is better captured; but its color is off as the whole BRDF slice takes on a reddish tint. Belcour’s models capture the lobe shape accurately at normal incidence, while their shape starts to depart from the reference at grazing incidences.

Transparent slabs Only the forward model of Belcour accommodates this category of materials. We do not use the tables *FGD* or *TIR*. In Figure 4, we show results for a smooth-on-rough yellow-tinted slab. The main transmitted lobe exhibits a relatively sharp falloff, likely due to total internal reflection at critical angles inside the slab; while a secondary, more colored lobe appears towards grazing angles, due to inter-reflections. Belcour’s model matches the reference lobe shape and color around normal incidence, except for the lobe tails that should be less pronounced. However, at grazing angles, its shape departs from the reference, as well as its direction; the second colored lobe is not present.

4. Analysis

4.1. Variants of Weidlich and Wilkie’s model

Both variants of Weidlich and Wilkie’s model [WW07] overestimate the intensity of the base layer which should be instead under-estimated as inter-reflections are not handled. It is due to the differential solid angle that should be modified. In Equation 2, this term is simply $\frac{1}{\eta_1^2}$ (see [Ish78][pp. 154]).

For plastic materials, the variant of Weidlich and Wilkie [WW09] exhibits angular variations of colors and intensity, especially pronounced at grazing angles (see Figure 1). These are due to the use of \mathbf{h}_0 to compute the transmitted directions $(\mathbf{l}_1, \mathbf{v}_1)$, leading to more absorption in this case of a yellow-tinted coating. For metallic materials, the model exhibits an additional lobe toward grazing angles (see Figure 2), due to the base layer BRDF f_{r1} being evaluated at too grazing angles. In comparison, the variant of Elek [Ele10] is devoid of these limitations as it properly uses the refracted directions $(\mathbf{l}_1, \mathbf{v}_1)$ to evaluate f_{r1} .

Both variants choose \mathbf{h}_0 to evaluate the transmissivity T_{01} , which does not make physical sense when the top layer is smooth. We suggest another variant that uses the geometric normal \mathbf{n} in the computation of both T_{01} and $(\mathbf{l}_1, \mathbf{v}_1)$:

$$f_r^{ww'}(\mathbf{l}_0, \mathbf{v}_0) = f_{r0}(\mathbf{l}_0, \mathbf{v}_0) + T_{01} f_{r1}(\mathbf{l}_1, \mathbf{v}_1) \frac{a}{\eta_1^2} T_{10}, \quad (4)$$

where a is the same as in Equation 2, the *TIR* term is removed and Elek’s roughness modification is used. This variant still remains limited as illustrated in Figures 5 and 6: inter-reflections in media are not considered; the roughness modification is not sufficient to account transmission through a rough interface; and finally, BTDFs are not handled.

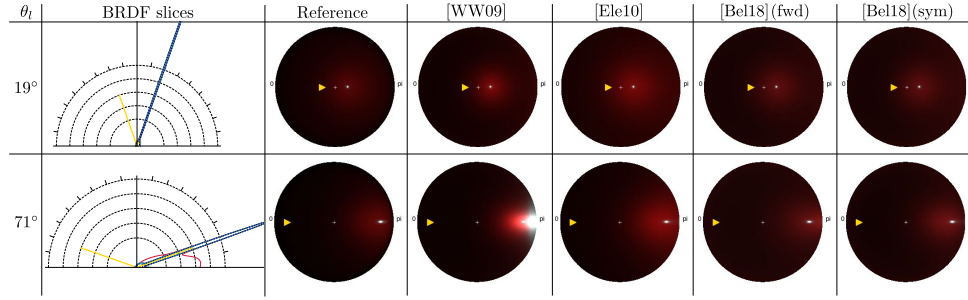


Figure 2: Results for a metallic paint material ($\alpha_0 = 0.001$, achromatic τ , $\alpha_1 = 0.2$, $\eta_1 = 1.45$). Four models are drawn in BRDF slice diagrams (red [WW09], orange [Ele10], cyan [Bel18](fwd) and blue [Bel18](sym)). The model of Weidlich and Wilkie exhibits artifacts at grazing angles; all other models only slightly differ in the extent of the wide redish reflection lobe.

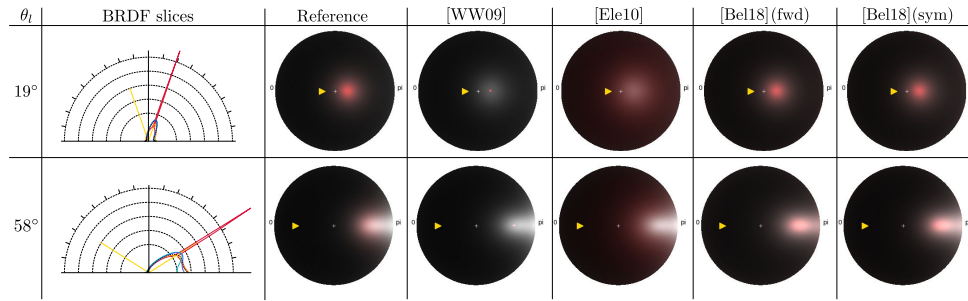


Figure 3: Results for a frosted metal material ($\alpha_0 = 0.2$, achromatic τ , $\alpha_1 = 0.001$, $\eta_1 = 1.45$). Weidlich and Wilkie's model cannot reproduce the redish rough reflection lobe. The variant of Elek captures the shape of that lobe, but not its color. Belcour's models accurately reproduce the lobe shape at normal incidence, but it departs from the reference toward grazing angles.

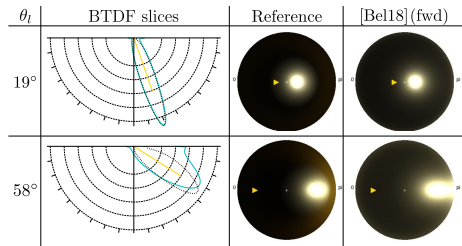


Figure 4: Results for a transparent slab material ($\alpha_0 = 0.001$, $\alpha_1 = 0.2$, colored τ). The model of Belcour [Bel18] (cyan) accurately captures the shape of the transmitted lobe around normal incidence (the lobe tails are less pronounced in the reference). The lobe shape departs significantly from the reference toward grazing angles: it is wider, points in a different direction, and does not reproduce the orange lobe.

4.2. Belcour's models

As shown in Section 3.2, the models of Belcour [Bel18] depart from the reference simulation mainly toward grazing angles. In metallic materials, the reflection off the top interface is approximate at grazing angles, especially with a rough coating. As seen in the BRDF slices of Figures 3,

the symmetric variant is slightly more accurate than the forward. This departure from the reference is likely due to the approximation made by the FGD term, which is based on \mathbf{h}_0 instead of \mathbf{n} for the symmetric variant. Regarding lobe colors, the forward variant produces desaturated colors at grazing angles, whereas the symmetric variant slightly overestimates saturation (see Figure 3); this is most likely due to the approximation brought by the FGD term, this time on transmission. Regarding lobe shapes, both variants produce reflections off the base layer that are wider compared to the reference, which we attribute to the projection of BRDF lobes on GGX-based functions.

In slab materials, the difference in lobe shapes is more pronounced (see Figure 4). At normal incidence, refracted lobes have stronger tails in Belcour's model compared to the reference, again due to projection on GGX lobes. Toward grazing angles, the shape of the refracted lobe departs even more from the reference. This is likely due to the multiple approximations accumulation with successive transmission events: the conversion between roughness and lobe variance, the "fake" rough refraction, etc. The direction of lobes also differ, which is due to the lack of updating mechanism for mean statistics; as a result, reflected and refracted lobes always point in the specular direction. Finally, the orange

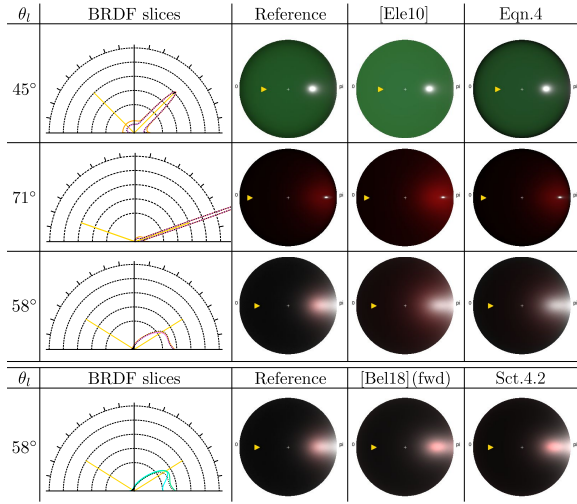


Figure 5: The variant of Equation 4 (pink) provides more accurate results for plastics (first row) and metallic paints (second row) than Elek’s. For frosted metals (third row), they significantly depart from the reference. The simple modification of Belcour’s model (Section 4.2, in green) systematically improves its accuracy, here for frosted metals (last row).

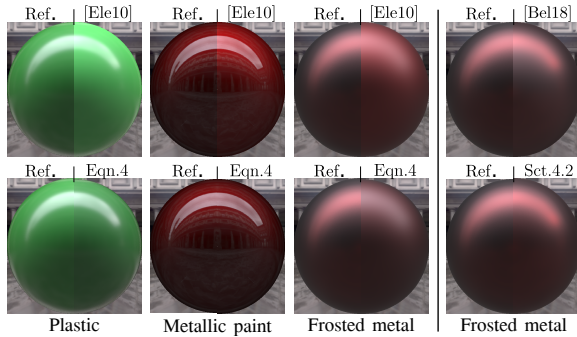


Figure 6: The differences of BRDF in Figure 5 are visible in renderings. Equation 4 is closer to the reference for plastics, indiscernible from the simulation for metallic paints, but inadequate for frosted metals. Belcour’s forward model modified as in Section 4.2 brings it closer to the reference.

secondary lobe observed in the reference is absent from the model results. This issue could be addressed by letting Belcour’s model output two lobes in this case; however, they would still be based on GGX functions and hence would depart from the reference lobe shape in this case.

We propose a trivial fix for issues found in reflection off the top interface, simply consisting in using f_{r0} for the 0-th lobe and Belcour’s forward variant for the next layers. As shown in Figures 5 and 6 for frosted metals, the reflection off the first interface is corrected, the effect is very similar on metallic patinas, but much more subtle on metallic paints.

5. Conclusion

We have conducted a numerical evaluation of two families of analytical BSDF models on layered material configurations organized in three categories: plastics, metals and transparent slabs. The two variants of Belcour [Bel18] have yielded the most accurate results for metals. Moreover, dealing explicitly with reflection off the top layer corrects some issues observed at grazing angles. Nevertheless, the model still departs from the reference in terms of lobe colors and shapes at grazing angles. Even though the two variants of Weidlich and Wilkie’s model [WW09, Ele10] are less accurate, we have shown that with a few corrections, the approach yields exact results on some materials. It would thus be interesting to investigate whether the two approaches could be combined in a model that could accommodate all materials.

References

[Bel18] BELCOUR L.: Efficient rendering of layered materials using an atomic decomposition with statistical operators. *ACM Trans. Graph.* 37, 4 (July 2018), 73:1–73:15. 1, 2, 4, 5

[BPB19] BATI M., PACANOWSKI R., BARLA P.: Numerical analysis of layered material models, 2019. 1

[Ele10] ELEK O.: Layered materials in real-time rendering. In *Central European Seminar on Computer Graphics* (2010), CESC10. 2, 3, 4, 5

[GHZ18] GUO Y., HAŠAN M., ZHAO S.: Position-free monte carlo simulation for arbitrary layered bsdfs. *ACM Trans. Graph.* 37, 6 (2018). 1

[QGQ17] GUO J., QIAN J., GUO Y., PAN J.: Rendering thin transparent layers with extended normal distribution functions. *IEEE Transactions on Visualization & Computer Graphics* 23, 9 (Sept. 2017), 2108–2119. 1

[Ish78] ISHIMARU A.: *Wave Propagation and Scattering in Random Media*. No. v. 2 in IEEE/OUP series on electromagnetic wave theory. Academic Press, 1978. 3

[JdJM14] JAKOB W., D’EON E., JAKOB O., MARSCHNER S.: A comprehensive framework for rendering layered materials. *ACM Trans. Graph.* 33, 4 (July 2014), 118:1–118:14. 1

[NDM05] NGAN A., DURAND F., MATUSIK W.: Experimental analysis of brdf models. In *Proceedings of (2005), EGSR ’05*. 1

[TS67] TORRANCE K. E., SPARROW E. M.: Theory for off-specular reflection from roughened surfaces*. *J. Opt. Soc. Am.* 57, 9 (Sep 1967), 1105–1114. 2

[WMLT] WALTER B., MARSCHNER S. R., LI H., TORRANCE K. E.: Microfacet models for refraction through rough surfaces. 1

[WW07] WEIDLICH A., WILKIE A.: Arbitrarily layered microfacet surfaces. In *Proceedings of the 5th International Conference on Computer Graphics and Interactive Techniques in Australia and Southeast Asia* (2007), GRAPHITE ’07, ACM, pp. 171–178. 1, 2, 3

[WW09] WEIDLICH A., WILKIE A.: Exploring the potential of layered brdf models. In *ACM SIGGRAPH ASIA 2009 Courses* (2009), SIGGRAPH ASIA ’09, ACM, pp. 7:1–7:58. 2, 3, 4, 5

[WW11] WEIDLICH A., WILKIE A.: Thinking in layers: Modeling with layered materials. In *SIGGRAPH Asia 2011 Courses* (2011), SA ’11, ACM, pp. 20:1–20:43. 2

[Yeh05] YEH P.: *Optical Waves in Layered Media*. Wiley Series in Pure and Applied Optics. Wiley, 2005. 1